N92-21608

EFFECT OF SHOCK PRESSURE ON THE STRUCTURE AND SUPERCONDUCTING PROPERTIES OF Y-Ba-Cu-O IN EXPLOSIVELY FABRICATED BULK METAL-MATRIX COMPOSITES.

L. E. Murr, C. S. Niou, and M. Pradhan-Advani

Department of Metallurgical and Materials Engineering
The University of Texas at El Paso
El Paso, Texas 79968-0520 USA

Abstract

Explosively fabricated or shock-wave processed $YBa_2Cu_3O_x$ exhibits a resistance-temperature signature characterized by a semiconducting normal-state behavior and a superconducting transition which is broadened with increasing shock pressure. The relative susceptibility (χ/χ_o) decreases with pressure while characteristic X-ray split-peak broadening is increased. Recovery of superconductivity requires thermal treatment in oxygen at temperatures above 900°C. Transmission electron microscope observations have revealed defect clusters having large, associated strain fields, apparently created by discontinuities in the shock front. A comparison of shock pressure effects with oxygen order-disorder phenomena and radiation (ion, electron, and neutron) effects illustrates the potential for controlling the resistance-temperature signature and the transport supercurrent density through flux pinning microstructures which optimize the explosive fabrication process and the residual superconductor behavior.

Introduction

While it is now well established that copper-oxide-based powder, or virtually any other ceramic superconductor powder, can be consolidated and encapsulated within a metal matrix by explosive consolidation (1-4), the erratic superconductivity following fabrication has posed a major problem for bulk applications of $YBa_2Cu_3O_7$. The nature of this behavior seems to arise from microstructural damage resulting from defects created in the shock front (5,6). Murr, et al. (3,7) have shown that the microtwin density in $YBa_2Cu_3O_7$ increases by an order of magnitude following explosive fabrication of superconducting powder at pressures of 4 to 8 GPa (6).

In this investigation we have examined the effects of shock pressure on the residual superconducting behavior of explosively fabricated bulk composites, principally the resistance versus temperature curve and the effects that heat treatment can have on restoring degraded superconductivity. The effect of shock pressure on residual susceptibility, and the relationship of shock-induced degradation to residual microstructure, especially shock-induced microstructure are also examined.

These features are implicit in systematic peak broadening of

characteristic X-ray spectra or observed directly by transmission electron microscopy. We also examine the implications of these observations in the context of related alterations (and degradation) of superconductivity by a variety of radiation treatments (8-12), elemental substitutions (13), and variations in oxygen content (14).

Experimental Considerations and Results

The details of explosive (shock-wave) fabrication of Y-Ba-Cu-O powder and the shock loading of sintered Y-Ba-Cu-O bulk samples have been given elsewhere (1-3,5,15). Conformal channels milled into a base plate are filled with superconducting Y-Ba-Cu-O powder prepared by a solid-state route described previously (3), and a cover plate is fitted into the channel to contain and pre-compress the powder. The flyer or cladding plate is then explosively welded to the base plate, simultaneously consolidating the powder, bonding it to the channel, and creating a monolithic composite. The accompanying shock wave produces defects which alter the residual superconductivity. The fabricated Y-Ba-Cu-O channel was removed from the metal or alloy monolith, and a four-probe electrode configuration attached using silver paste. The R-T signatures were measured using a standard test current of 10 mA. Coupons of sintered Y-Ba-Cu-O were subjected to a 6 GPa shock pulse (5). The samples were recovered and the resistance versus temperature curve measured as described above.

We have also measured the microwave surface resistance (R_s) for Y-Ba-Cu-O superconducting powder following explosive fabrication and after heat treatment. A resonant microstrip technique was used (16) and compared with a copper reference sample at the same resonant frequency. Figure 1 shows an example of a prototype from which

FIG. 1: Example of explosively fabricated, monolithic prototype showing a milled section exposing superconducting channels in Al-6061-T6 tooling plate.

samples have been extracted for R_s measurements, as well as other measurements (including supercurrent density). In the example shown in Fig. 1, the base plate was an aluminum 6061-T6 alloy, the cover plates were silver, and the cladding plate was copper. The copper clad plate and cover plates have been milled away to expose the Y-Ba-Cu-O consolidated powder channel strips.

Figure 2(a) shows the as-fabricated, resonant microwave surface resistance values (R_s) compared with several other experimental measurements at liquid nitrogen temperature (77K). In addition, Fig. 2(a) also shows the annealed R_s value, the bulk d.c. resistance ($R_{d.c.}$) following explosive fabrication, and the annealed, bulk superconductivity (zero resistance) from Fig. 2(b) and (c). The dotted line in Fig. 2(a) corresponds to the bulk resistance at 77K (in liquid nitrogen). It is of interest to note in Fig. 2(a) that while the R_s value for copper increases in the microwave regime in comparison to the bulk, d.c. (zero frequency) regime, the as-fabricated Y-Ba-Cu-O resistance actually decreases ($R_s < R_{d.c.}$). On the other hand, $R_{d.c.}$ (=0) < R_s (=16 mΩ) for the annealed, superconducting Y-Ba-Cu-O (Fig. 2(b)).

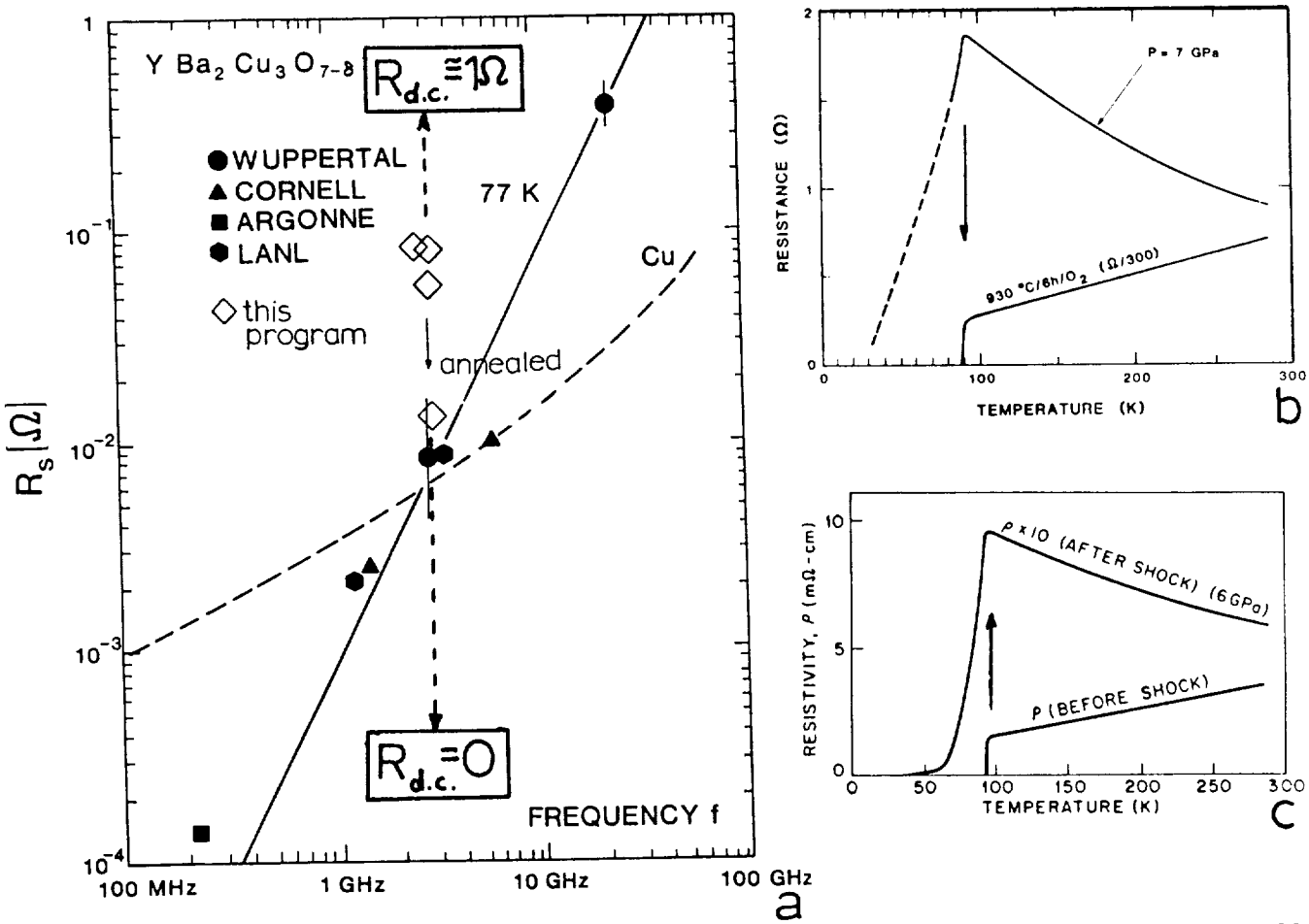

FIG. 2: Comparison of resonant microwave surface resistances and bulk resistance values along with other laboratory data for Y-Ba-Cu-O (a) with shock consolidated and annealed powder (b) and plane-wave shock loaded sintered coupons (c).

We examined the a.c. magnetic susceptibility ($-4\pi\chi$) by regrinding samples of explosively consolidated channel sections extracted from the monolithic composites illustrated in Fig. 1 to the same size and size distribution of the starting powder and pressing these powders into cylindrical pellets having a green density of ~65%. These experimental pellets were then measured along with the starting, unfabricated powder pellets, to obtain relative susceptibility ratios (χ/χ_o); where χ_o is the susceptibility for the unfabricated (unshocked) powder. In addition, portions of the reground powder samples, as well as the unfabricated powders, were examined by X-ray diffraction spectrometry (Cu-Kα radiation), and characteristic, orthorhombic split-peak signatures (corresponding to $2\theta \cong 32^\circ$ and 58°) as discussed previously (4) were compared.

Figure 3 shows for comparison the measured relative susceptibilities and the ratios of X-ray peak broadening (for $\Delta 2\theta \cong 32^\circ$) as a function of shock pressure. It is apparent that there is a consistent and characteristic degradation of diamagnetic shielding (χ/χ_o) with increasing shock pressure. In addition, these results correspond to previous but higher shock pressure research by Morosin, et al. (17), and also correspond to increasing strain energy ($\Delta 2\theta/\Delta 2\theta_o$) consistent with higher densities of shock-induced defects.

We examined the unfabricated powders and sintered Y-Ba-Cu-O as well as the explosively fabricated and shock loaded Y-Ba-Cu-O (Fig. 2(c)) by argon ion milling (at 6keV) of mechanically ground and polished thin sections to produce electron transparent specimens which could be observed in the transmission electron microscope. A Hitachi H-800 analytical STEM was used at 200kV to perform a range of CTEM observations, including high-resolution lattice imaging.

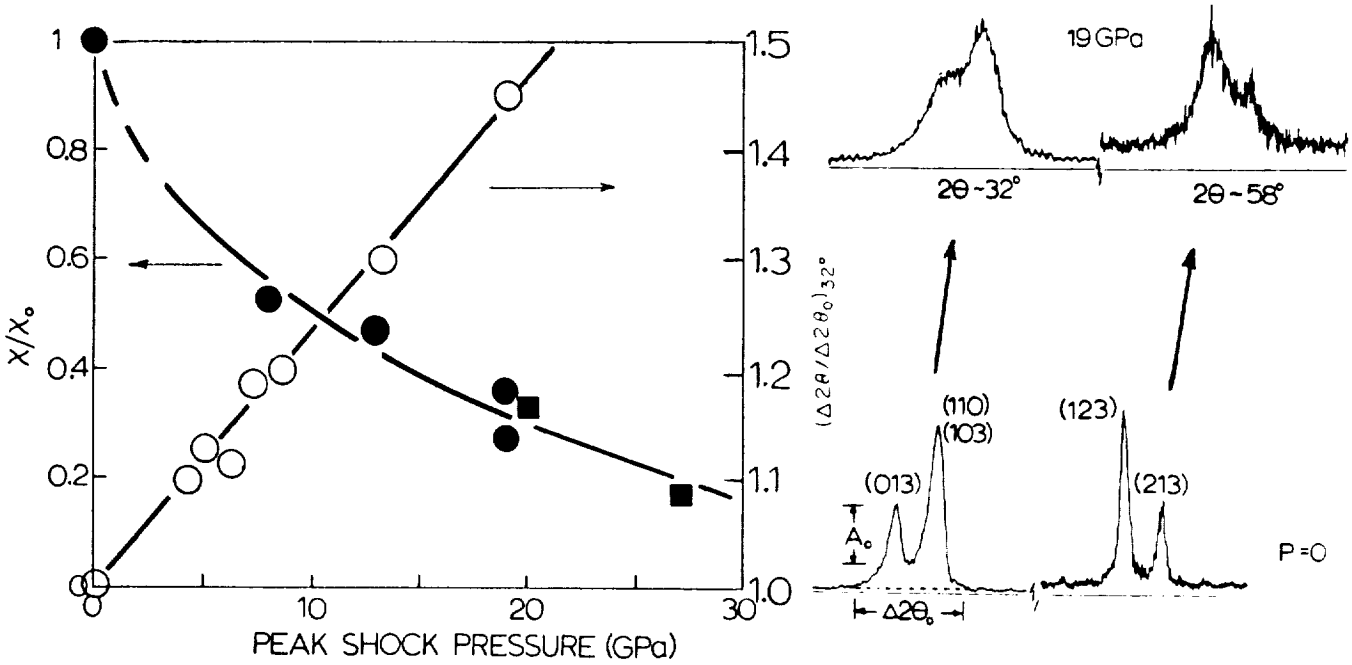

FIG. 3: Relative susceptibility and characteristic orthorhombic X-ray peak broadening ratio versus shock pressure. The data of Morosin, et al. (17) is shown for comparison as solid squares.

Figure 4 illustrates some examples of shock-induced defects which are observed in the explosively fabricated (Fig. 4(a)) as well as the plane-wave shock loaded material (Fig. 2(c)). These defects exhibit significant strain field contrast (Fig. 4(b)) which can phenomenologically account for the significant peak broadening (residual strain broadening) observed in the X-ray diffraction studies illustrated in Fig. 3. Furthermore overlapping strain fields could also phenomenalogically account for the complete lack of a superconducting transition by destroying the phase coherence of the superconducting pair wave function as alluded to in the work of White, et al. (18) where the phase coherence was destroyed by high fluence ion irradiation of $YBa_2Cu_3O_x$ films which produced microstructural damage created by what they described as nuclear-energy loss processes.

Discussion and Comparison of Shock-Pressure Effects

It is now well established that $YBa_2Cu_3O_{7-\delta}$, either as a thin film or bulk material, is very sensitive to defects, including subsitutional impurities (13), oxygen concentration, (8) (which variously alters the oxygen order-disorder phenomenon, particularly in the context of b-chain Cu-O periodicity (14,19)), and a host of irradiation effects (8-12,18).

These effects are illustrated for comparison with the effect of shock pressure and heat treatment in Fig. 5. An interesting feature about shock or explosive fabrication in contrast to oxygen deficiency or ion or electron irradiation is the fact that the T_c (onset) does not change with pressure or heat treatment. Recent work by van Dover, et al. (12) has indicated that the R-T signature (the transitional broadening) is not changed with neutron irradiation, while significant flux pinning raises the critical current density (as measured from magnetization changes) to a value near 10^6 A/cm^2. A feature observed in Fig. 5 is the rather consistent decrease in T_c (onset) for oxygen deficiency and electron and ion irradiation.

While there have not been any observations of defects in any irradiated samples (except for the early ion damage studies by Clark, et al. (8) which suggested the stimulated growth of an amorphous layer at the grain boundaries in thin films), it is apparent that the defects are different from those observed in Fig. 4. In addition, the effects or radiation may also differ in thin film and bulk materials not dominated by weak-link intergranular connections. It is obvious from Fig. 4 that the shock wave-induced defects are not simple atomic displacements but rather a cluster which resembles a precipitate (6), which is not easily annealed out (Fig. 5(a)). By comparison, the effects of electron and ion irradiation can often be annealed out at temperatures just above room temperature (8,10), suggesting simple displacements, even oxygen displacements from the Cu-O chains may be involved.

It is generally accepted that the ordering of the Cu-O chains is essential for superconductivity in the $YBa_2Cu_3O_7$ (or $YBa_2Cu_3O_x$), especially the so-called chain planes (the basal planes in the unit cell)(14,19,20). In fact, as illustrated schematically in Fig. 6, subtracting only one oxygen from the unit cell of $YBa_2Cu_3O_7$ produces a

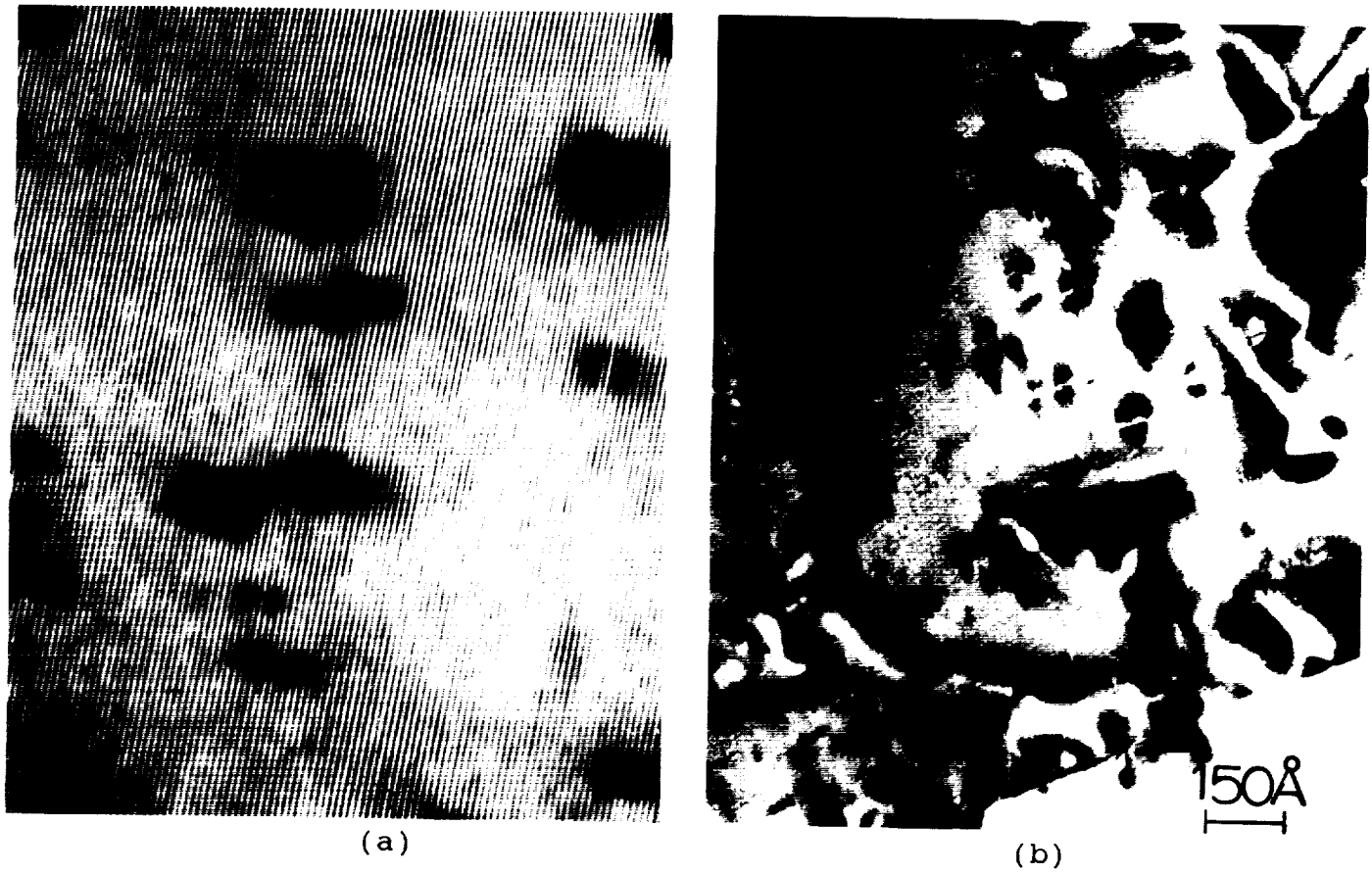

FIG. 4: Defect clusters with associated strain field contrast observed in explosively fabricated and shocked Y-Ba-Cu-O. (a) shows lattice image viewed along the b-chains [010] after explosive fabrication at 7 GPa. (b) Strain-field contrast of defects in plane-wave shock loaded Y-Ba-Cu-O at 6 GPa.

nonsuperconducting, semiconducting (or semi-insulating) material ($YBa_2Cu_3O_6$). Figure 6 also shows the structural variances which can occur for specific oxygen stoichiometries between the superconducting, orthorhombic $YBa_2Cu_3O_7$ and the nonsuperconducting, tetragonal $YBa_2Cu_3O_6$, where the transitional stoichiometries at x = 6.75, 6.5, and 6.25 correspond roughly to the distinctions in the oxygen R-T signatures shown in Fig. 5(b). Figure 7 also elaborates the Cu-O b-chain periodicities which, along with the oxygen order-disorder can account for shifts in the T_c (onset) as well as variations in the normal state resistance (or resistivity)(Fig. 5(b)). The oxygen in the chains (Fig. 7) is the weakest bound of the elemental species in Y-Ba-Cu-O and is easily removed even by thermal treatment (19). Such displacements can also account for the creation of microtwins by systematic displacement of oxygen on the b axis to interstitial locations on the a axis. Indeed there is an increase in microtwin density with explosive processing at lower pressures (4 to 8 GPa)(3) and there is no apparent oxygen loss (5).

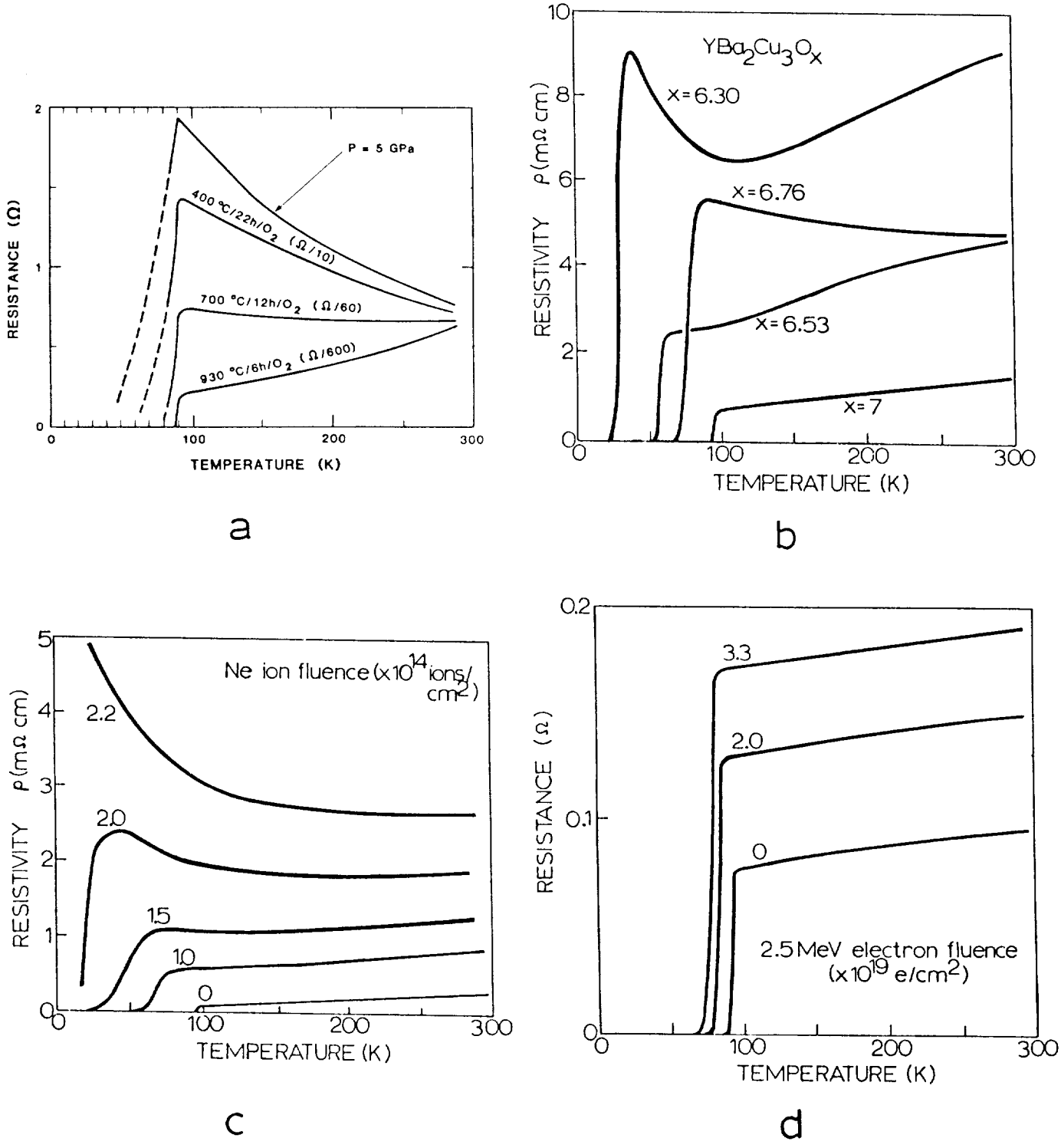

FIG. 5: Comparison of resistance-temperature signatures for shock fabricated and heat treated Y-Ba-Cu-O (a) with those for oxygen (x) deficient (b), ion irradiated (c), and electron irradiated (d) Y-Ba-Cu-O. Data reproduced in (b), (c), and (d) is after references (14), (9), and (10) respectively.

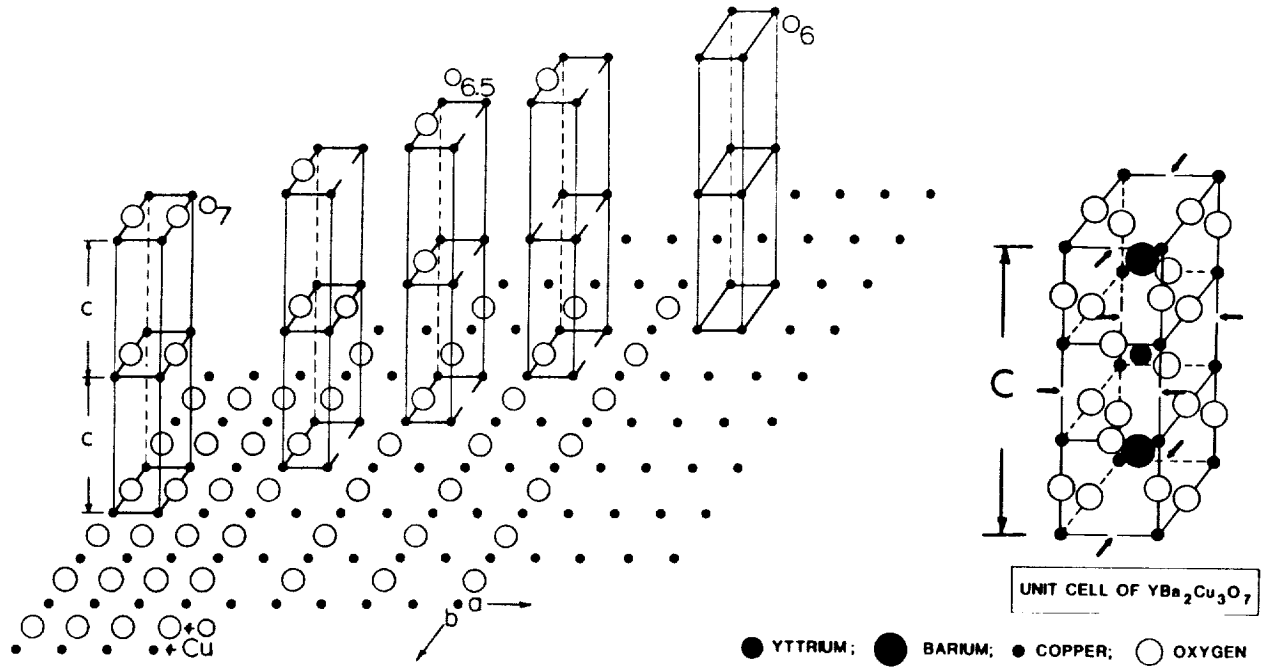

FIG. 6: Basal-plane oxygen (vacancy) order-disorder along b-chains (b-axis) and Cu-O chain periodicity with oxygen content. The double unit cell variances produce variations in b-chain periodicities as shown.

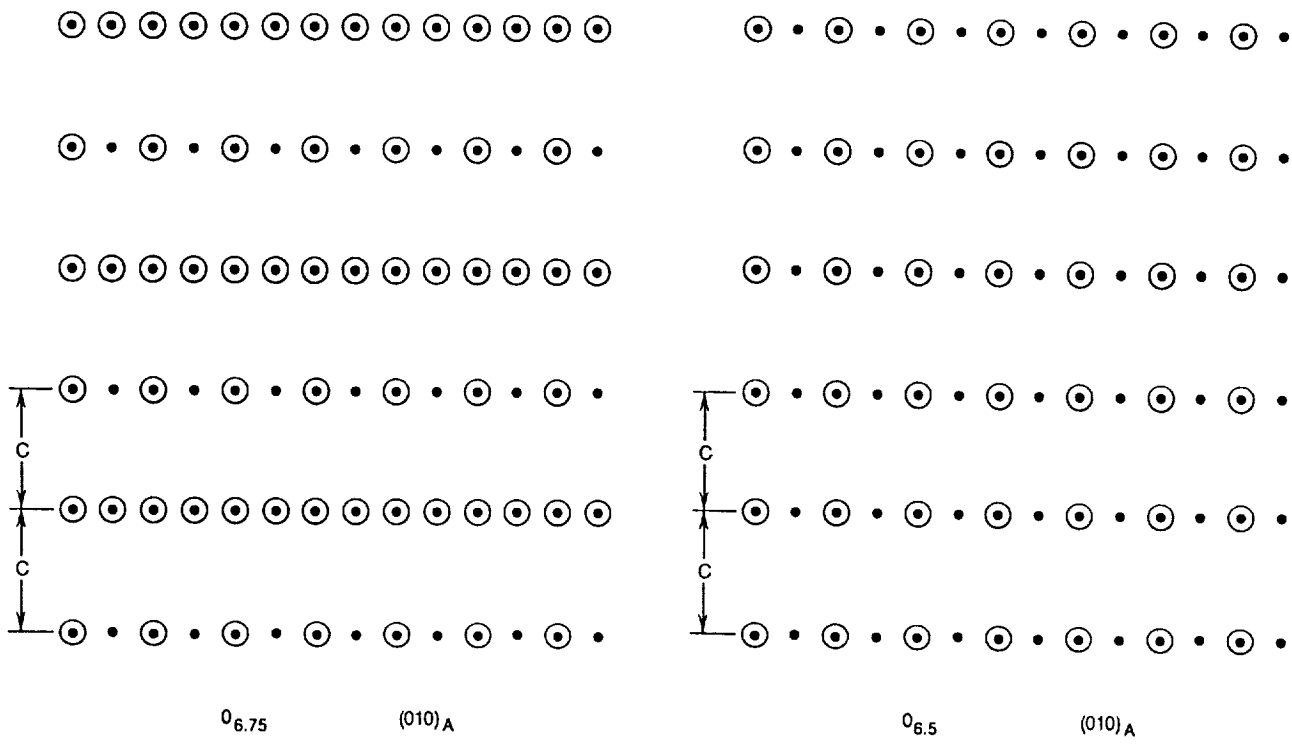

FIG. 7: Schematic views of b-chain periodicities viewed in the b-axis direction (Fig. 6). Solid circles are copper, open circles are oxygen. These views show oxygen vacancy periodicity in the b-chain.

In the context of granularity, macroscopic resistivity is strongly influenced by each grain or microstructural domain which contributes to a partial path across the sample, creating a kind of percolation, with the zero resistance state occurring at or near the percolation threshold (21). However, in bulk superconductors the zero resistance paths can be along the surface, and this phenomena can at least account in principle for the anomalous resistance difference illustrated in Fig. 2(a) which in effect compares the bulk ($R_{d.c.}$) percolation resistance with the surface, microwave resistance (R_s) at constant temperature (77K). This difference may also reflect the relaxation of strain fields or defects near the surface as well.

Conclusions

It is clear from Figs. 5 and 6 that the atomic ordering, and even the ordering of Cu-O chains as suggested in Fig. 7, as well as a variety of crystal defects, have a controlling influence not only on the superconducting transition and the transition temperatures, but also on the normal-state resistance behavior as well. The shape of the R-T curve might therefore be manipulated by a clear understanding of the role that specific defects can play, and their interaction to produce specific resistance-temperature signatures, and flux pinning to accomodate large supercurrent transport densities.

It may be possible to manipulate the microstructure of the starting superconducting powder to optimize the R-T signature as well as the flux pinning properties so that both are enhanced following explosive fabrication. Jin, et al. (22) have in fact recently demonstrated that intragranular flux pinning could be enhanced by fine-scale defects (similar to those shown in Fig. 4) produced by rapid decomposition of the $YB_2Cu_4O_8$ precursor to superconducting Y-Ba-Cu-O. While the shock wave might alter the nature of such defects or create new or additional defects, the residual microstructures might produce a different R-T signature than those shown in Fig. 2(b) and (c) and Fig. 5(a). In effect, it may be possible to take advantage of atomic-scale distortions by tailoring the starting materials microstructures and optimizing the explosive fabrication process by adjusting the shock pressure without compromising the cladding of the metal matrix assembly. This will require a more concerted effort to systematically examine a wide range of microstructures by transmission electron microscopy.

Acknowledgements

This research is supported by the DARPA HTSC Program under Contract ONR-N00014-88-C-0684, and in part by NASA(Goddard)-SBIR Contract NAS5-30504 through Monolithic Superconductors, Inc. We thank Dr. L. H. Schoenlein for his help with some of the electron microscopy analysis and Dr. Wayne Bongianni for his help in measuring the resonant microwave resistances.

References

1. L. E.Murr, A. W. Hare, and N. G. Eror, Nature, 329, 37(1987).
2. L. E. Murr, N. G. Eror, and A. W. Hare, SAMPE J., 24(6), 15(1988).
3. L. E. Murr, T. Monson, J. Javadpour, M. Strasik, U. Sudarsan, N. G. Eror, A. W. Hare, D. G. Brasher, and D. J. Butler, J. Metals, 40(1), 19(1988).
4. L. E. Murr and N. G. Eror, Materials & Manufacturing Processes, 4(2), 177(1989).
5. L. E. Murr, C. S. Niou, S. Jin, T. H. Tiefel, A. C. W. P. James, R. C. Sherwood, and T. Siegrist, Appl. Phys. Lett., 55(15), 1575(1989).
6. L. E. Murr, M. Pradhan-Advani, C. S. Niou, and L. H. Schoenlein, Solid State Comm., in press (1990).
7. L. E. Murr, T. Monson, M. Strasik, U. Sudarsan, N. G. Eror, and A. W. Hare, J. Superconductivity, 1(1), 3(1988).
8. G. J. Clark, A. D. Marwick, R. H. Koch, and R. B. Laibowitz, Appl. Phys. Lett. 51, 139(1987).
9. J. M. Valles, A. E. White, K. T. Short, R. C. Dynes, J. P. Garno, A. F. J. Levi, M. Anzlowar, and K. Baldwin, Phys. Rev. B., 39(16), 11,599(1989).
10. H. Vichery, F. Rullien-Albenque, H. Pascard, M. Konczykowski, R. Kormann, D. Favrot, and G. Collin, Physica C, 159, 697(1989).
11. A. Umezawa, G. W. Crabtree, J. Z. Liu, H. W. Weber, W. K. Kwok, L. H. Nunez, T. J. Moran, and C. H. Sowers, Phys. Rev. B., 36(13), 7151(1987).
12. R. B. van Dover, E. M. Gyorgy, L. F. Schneemeyer, J. W. Mitchell, K. V. Rao, R. Puzniak, and J. V. Waszczak, Nature, 342 55(1989).
13. G. Xiao, F. H. Streitz, A. Garvin, Y. W. Du, and C. L. Chien, Phys. Rev. B, 35, 8782(1987).
14. R. J. Cava, B. Batlogg, L. H. Chen, E. A. Rietman, S. M. Zahurak, and R. Werder, Phys. Rev. B, 36, 5719(1987).
15. L. E. Murr, C. S. Niou, and M. Pradhan-Advani, to be published (1990).
16. J. L. Archer, W. C. Bongianni, and J. H. Collins, J. Appl. Phys., 41(3), 1359(1970).
17. B. Morosin, R. A. Graham, E. L. Venturini, and D. S. Ginley, Proc. 2nd Workshop on Industrial Application Feasibility of Dynamic Composition Technology, Tokyo Institute of Technology, Dec. 1-2, 1988, p. 97.
18. A. E. White, K. T. Short, D. C. Jacobson, J. M. Poate, R. C. Dynes, P. M. Mankiewich, W. J. Kocpol, R. E. Howard, M. Anzlowar, K. W. Baldwin, A. F. J. Levi, J. R. Kwo, T. Hsich, and M. Hong, Phys. Rev. B, 37(7), 3755(1988).
19. G. Van Tendeloo, H. W. Zandbergen, and S. Amelinckx, Sol. St. Comm., 63, 389(1987).
20. T. Siegrist, S. Sunshine, D. W. Murphy, R. J. Cava, and J. M. Zuhurak, Phys. Rev. B, 35, 7137(1987).
21. D. C. Larbalestier, M. Daeumling, P. J. Lee, T. F. Kelly, J. Seuntjens, C. Meingast, X. Cai, J. Mckinnell, R. D. Ray, R. G. Dillenburg, and E. E. Hellstran, Cryogenics, 27, 411(1987).
22. S. Jin, T. H. Tiefel, S. Nakahara, J. E. Graebner, H. M. O'Bryan, R. A. Fastnacht, and G. W. Kammlott, Appl. Phys. Lett., in press (1990).